Metrol. Meas. Syst., Vol. 31 (2024) No. 1, pp. 3–21
DOI: 10.24425/mms.2024.148543

PAN POLSKA AKADEMIA NAUK

METROLOGY AND MEASUREMENT SYSTEMS
Index 330930, ISSN 0860-8229
www.metrology.wat.edu.pl

M&MS

CYLINDRICAL GEAR TRANSMISSION ERRORS INFLUENCED BY TEMPERATURE BASED ON THERMAL NETWORK

Jie Tang[1,2)], Heng Guo[1)], Hui Wan[1)]

1) Faculty of Materials and Manufacturing, Beijing University of Technology, 100124 Beijing, China
(✉ *tangjie@bjut.edu.cn*)
2) Beijing Engineering Research Center of Precision Measurement Technology and Instruments, 100124 Beijing, China

Abstract

Gear transmission errors are influenced by temperature especially in the aerospace field. A model is proposed to investigate the influence of temperature on cylindrical gear transmission errors based on the thermal network (TETN). The gear temperature field distribution model is established based on the thermal network method, and gear thermal deformation can be calculated along the gear meshing line. Regarding the gear single-flank rolling process, the variation of gear transmission errors under temperature is determined. In numerical calculations in MATLAB, the variation of gear transmission errors at 100°C compared to 20°C is –4.20 μm, which decreases almost linearly while the thermal expansion coefficient of the gear material increases. The simulation of the gear transmission errors variation of temperatures using the finite element method (FEM) were carried out in Workbench software under Ansys and the average difference of the TETN model results between calculations and FEM for different temperatures was 0.24 μm. Experiments were carried out on the gear tester in temperatures ranging from 0°C to 100°C, the TETN model results in calculations were compared with the results of the tester, and the average difference was –1.15 μm. The results show that the proposed TETN can be used as an algorithm to determine the variation of gear transmission errors under the influence of temperature.

Keywords: cylindrical gear, temperature, thermal network, transmission errors.

1. Introduction

Transmission error is the error between the actual rotation angle and the theoretical rotation angle of the gear on the output shaft when the gear pair is engaged in single-flank at a certain distance from the center [1]. Transmission error is related to multiple deviations such as pitch deviations, which directly affect the noise and service life of the entire system [2]. The gear rolling process is affected by many factors, such as tooth surface accuracy and temperature, *etc*.

The gear temperature field consists of flash temperature and bulk temperature in rotation. Blok [3] presented the history of the flash temperature concept and the formulas for calculating

Article history: received May 6, 2023; revised August 8, 2023; accepted September 16, 2023; available online February 14, 2024.

flash temperatures. Taburdagitan and Akkok [4] simulated the flash temperature using the finite element software by calculating the frictional heat and the convection heat transfer coefficient. They found that the highest temperature is within the initial contacts. Li and Anisetti [5] investigated the flash temperature rises of spur gear, which are quantified within a wide speed range. Mao [6] analyzed flash temperature using the finite difference method, and the resulting mean value of flash temperature conformed with the Blok flash temperature criterion.

Li *et al.* [7] developed the simulation of a heat generation process of friction in the involute gears engagement in Ansys in which the bulk temperature and flash temperature were analyzed. Shi *et al.* [8] established a gear bulk temperature field and gear transient temperature filed model using FEM. Wang *et al.* [9] analyzed the bulk temperature of the anti-backlash single-roller enveloping an hourglass worm gear using Ansys to find the main factors causing temperature rise. Yi and Quinonez [10] measured real-time gear surface temperature variations under a wide range of operating conditions, and found that the maximum temperature occurs near the dedendum circle. Miltenovic *et al.* [11] calculated the temperature distribution of a worm gear using FEM based on the power loss data. Roda–Casanova and Sanchez–Marin [12] simulated a frictional heat generation process during gear meshing using a heat flux function based on a 2D FEM model to obtain the temperature field. Li *et al.* [13] calculated the frictional heat flux and convective heat transfer coefficient, and simulated the related gear temperature field.

The majority of the research work above uses FEM to obtain gear temperature field. In the thermal network method [14], a number of temperature nodes are arranged on the measurand, temperature is considered as voltage, heat flow is regarded as a current, each temperature node is connected by thermal resistance, the incoming heat flow of each temperature node is equal to the outcoming heat flow. Zhou *et al.* [15] established a thermal network temperature field model to predict the contact temperature of cylindrical spur gears, and thus the gear bulk and flash temperatures are obtained.

Thermal deformation will occur under the influence of temperature according to the thermal expansion and contraction characteristics of the gear material. Wiemann *et al.* [16] analyzed the influence of thermal expansion on the gear profile and helix deviations of *Physikalisch-Technische Bundesanstalt's* (PTB's) large gear measurement standards The results of a 3D scatter linear model for involute gears thermal expansion are compared to ones obtained via the finite element analysis as well as the experimental results by a *coordinate measuring machine* (CMM). Wang *et al.* [17] measured the temperature of instantaneous meshing points on the tooth surface, and these discrete temperature values are fitted by linear interpolation to establish the temperature distribution along gear radial direction, and then the gear thermal deformation is calculated. As gear thermal deformation under the influence of temperature lead to the variation of gear transmission errors, Trochta *et al.* [18] carried out the test these errors for different oil temperatures in the gear box, and established the linear relationship.

Gear transmission errors are analyzed mostly with FEM. There has been less research progress or fewer algorithms concerning the transmission errors under the influence of temperature for cylindrical gears. Wang *et al.* [19] analyzed the gear for body temperature field and calculated comprehensive deformation of the loaded gear by using the contact method, and the gear transmission error considering the thermal deformation was calculated.

This article aims at establishing the algorithm of influence of temperature on cylindrical gear transmission errors based on the thermal network method. After introducing the theoretical model, numerical simulation is performed at different temperatures and materials. Then the finite element simulation is performed using Ansys Workbench. Finally, experimental tests are carried out on a temperature tester to compare the experimental results with the simulation results.

Metrol. Meas. Syst., Vol. 31 (2024), No. 1, pp. 3–21
DOI: 10.24425/mms.2024.148543

2. Influence of temperature on gear transmission errors

2.1. The model of the influence of temperature on gear transmission errors

Gear transmission errors can be expressed by angle error or deformation along the meshing line. In Figure 1, Gear 1 is the driving gear and rotates counterclockwise, Gear 2 is the driven gear, M is the theoretical contact point of gear pair, M' is the actual contact point of the gear pair, φ_1 is the angle of Gear 1 where the theoretical contact position occurs, φ_2' is the angle of Gear 2 on the actual contact position. The deformation on the gear meshing line δ_N, which can be expressed as the gear transmission error, is described in (1), where i_c is the gear ratio and subscripts 1 and 2 represent Gears 1 and Gear 2 respectively.

$$\delta_N = r_{b2}\left(\varphi_2' - \frac{\varphi_1}{i_c}\right) = r_{b2}\varphi_2' - r_{b1}\varphi_1, \tag{1}$$

where r_{b1} is the base circle radius of Gear 1 (unit: mm), r_{b2} is the base circle radius of Gear 2 (unit: mm).

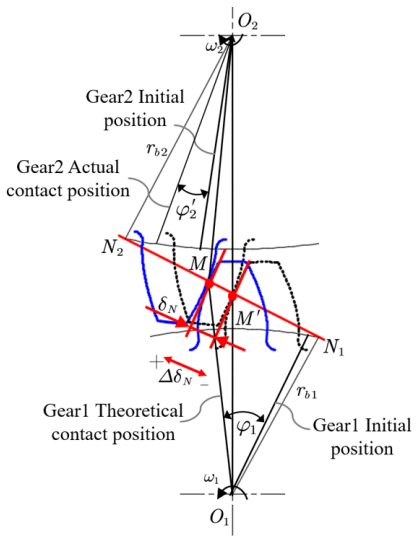

Fig. 1. Gear transmission error.

During the gear transmission process, the ambient temperature changes, at the same time, the gear contact stress and the relative sliding velocity of the gear may change too, which makes a difference in the gear temperature field. Then, thermal deformation occurs according to thermal expansion and contraction properties of the gear material, which affects the deformation on the gear meshing line. The deformation on the gear meshing line δ_N mainly includes two parts, as described in (2), where δ_T is the deformation on the gear meshing line caused by temperature, δ_E is the deformation on the gear meshing line caused by gear manufacturing accuracy, installation errors and other factors. Under conditions that keep the other factors unchanged, the variation on gear meshing line $\Delta\delta_N$ equals to $\Delta\delta_T$, which is shown in (3).

$$\delta_N = \delta_T + \delta_E \tag{2}$$

$$\Delta\delta_N = \Delta\delta_T \tag{3}$$

The gear single-flank meshing process is shown in Fig. 2, It is normally affected by the contact ratio of 1 to 2. In Fig. 2a, the gear enters the first double-teeth meshing area AB, at this period, the gears have two meshing points D' and A. In Fig. 2b, the gear leaves the first double teeth meshing area AB and enters the single-tooth meshing area BD, the two contact points are $E'$and B. In Fig. 2c, the gear enters the single-tooth meshing area BD, meanwhile the contact point is K. Along with the rotation, the gear enters the second double teeth meshing area DE, as shown in Fig. 2d, the contact points are D and A''. In Fig. 2e, the gear will be a part of the meshing, the contact points are E and B''.

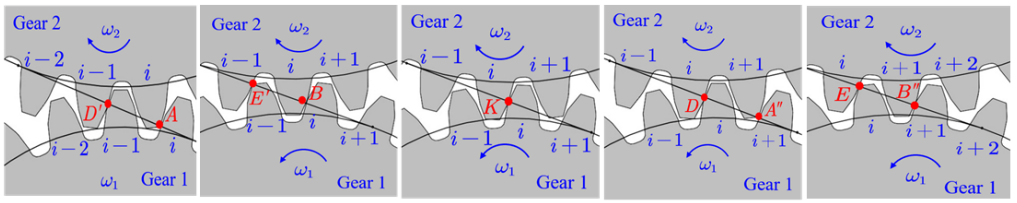

Fig. 2. Single-flank meshing process.

Considering the deformation of the gear meshing line caused by temperature, when the gear rotates from φ_A to φ_B, it is in the first double-teeth meshing area AB and two factors affect the deformation on gear meshing line δ_{Ta} caused by temperature, which are thermal deformation δ_{TAB} of the i-th pair of gear teeth from point A to point B and thermal deformation $\delta_{TD'E'}$ of the (i-1)th pair of meshing gears from point D' to point E'

Gears are in the single-tooth meshing area BD when rotating from φ_B to φ_D and only the i-th pair of gear tooth is in contact. Here, gear meshing line deformation δ_{Tb} caused by temperature can be obtained through calculating the i-th pair of gear teeth thermal deformation δ_{TBD}.

When the gear rotates from φ_D to φ_E, the gear is in the second double-teeth meshing area DE, and the deformation on gear meshing line δ_{Tc} caused by temperature can be determined by calculating the thermal deformation δ_{TDE} of the i-th pair of gear teeth from point D to point E and thermal deformation $\delta_{TA''B''}$ of $(i+1)$-th pair of meshing gear teeth from point A'' to point B''

The thermal deformation of each gear meshing area is shown in (4) where φ is the gear rotation angle. The deformations are described in (5) to (9).

$$\Delta\delta_T = \begin{cases} \delta_{Ta} = \delta_{TAB} + \delta_{TD'E'} & (\varphi_A < \varphi < \varphi_B) \\ \delta_{Tb} = \delta_{TBD} & (\varphi_B < \varphi < \varphi_D) \\ \delta_{Tc} = \delta_{TDE} + \delta_{TA''B''} & (\varphi_D < \varphi < \varphi_E) \end{cases}, \tag{4}$$

$$\delta_{TAB} = \delta_{1AB} + \delta_{2AB}, \tag{5}$$

$$\delta_{TD'E'} = \delta_{1D'E'} + \delta_{2D'E'}, \tag{6}$$

$$\delta_{TBD} = \delta_{1BD} + \delta_{2BD}, \tag{7}$$

$$\delta_{TDE} = \delta_{1DE} + \delta_{2DE}, \tag{8}$$

$$\delta_{TD''E''} = \delta_{1D''E''} + \delta_{2D''E''}. \tag{9}$$

where δ_{1AB}, δ_{2AB} is the thermal deformation of the meshing gear teeth from point A to point B of Gear 1 and Gear 2 respectively (unit: mm) $\delta_{1D'E'}$, $\delta_{2D'E'}$ is the thermal deformation of the meshing gear teeth from point D' to point E' of Gear 1 and Gear 2 respectively (unit: mm) and also the same definition for δ_{1BD}, δ_{2BD}; δ_{1DE}, δ_{2DE}; $\delta_{1A''B''}$, $\delta_{2A''B''}$.

Metrol. Meas. Syst., Vol. 31 (2024), No. 1, pp. 3–21
DOI: 10.24425/mms.2024.148543

2.2. The temperature field distribution

There are three ways of heat transfer: heat convection, heat conduction and heat radiation. Heat radiation in the gear temperature field is ignored in this work. In the steady state temperature field, the gear tooth temperature field can be equivalent to a cylinder with uniform temperature, and the temperature value is the ambient temperature. The bulk temperature field is addressed because the gear flash temperature has a small effect on the gear thermal deformation. Then the analysis of the gear tooth temperature field is performed.

The thermal network method can analyze the steady-state temperature field of gears. First, the heat transfer process of each gear tooth surface must be determined, as shown in Fig. 3. Different boundary conditions are obtained. After determining the heat transfer process of the gear, combined with the corresponding thermal resistance calculation of heat transfer and the thermal network method, the *temperature field distribution* model of the cylindrical gear based on the *thermal network method* (TFD-TN) can be established, as shown in Fig. 4.

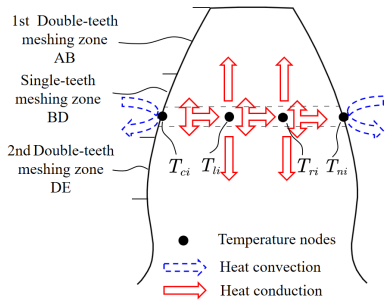

Fig. 3. Heat transfer process.

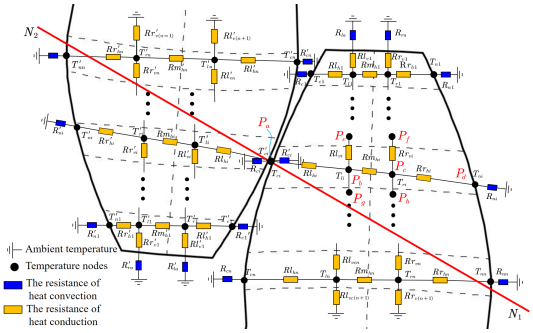

Fig. 4. Sketch map of gear temperature field distribution.

In this TFD-TN model, the tooth surface is divided into three areas from the tooth tip to the base circle according to the gear meshing process. Each part is discretised into several regions, and each discrete region has several temperature nodes. Each temperature node is connected by thermal resistance, and the inflow of heat from each temperature node through convection or heat conduction is equal to the outflow of heat conduction to other temperature nodes. An equation can be created for each temperature node, and several equations can be listed for each discrete region. Take four temperature nodes as an example, equations are expressed as (10) to (13). The equation established for the whole tooth surface is shown in (14).

$$Q_{1i}S_{1i} = \frac{T_{c1} - T_a}{R_{c1}} + \frac{T_{c1} - T_{l1}}{R_{lhi}}, \tag{10}$$

$$\frac{T_{ci} - T_{li}}{R_{lhi}} = \frac{T_{li} - T_{l(i-1)}}{R_{lvi}} + \frac{T_{li} - T_{ri}}{R_{mhi}} + \frac{T_{li} - T_{l(i+1)}}{R_{lv(i+1)}}, \tag{11}$$

$$\frac{T_{li} - T_{ri}}{R_{mhi}} = \frac{T_{ri} - T_{r(i-1)}}{R_{rvi}} + \frac{T_{ri} - T_i}{R_{rhi}} + \frac{T_{ri} - T_{r(i+1)}}{R_{rv(i+1)}}, \tag{12}$$

$$\frac{T_{ri} - T_{ni}}{R_{rhi}} = \frac{T_{ni} - T_a}{R_{ni}}. \tag{13}$$

In (10), the incoming heat flow generated by friction at temperature node P_a on the meshing tooth surface of the cylindrical gear is equal to the sum of the outcoming heat flow to the tooth space and the tooth body. Equations (11) or (12) are for the temperature node inside the tooth body

P_b or P_c, respectively, the incoming heat flow to this node from the meshing surface temperature node P_a or P_b is equal to the outcoming heat flow to other neighboring temperature nodes. In (13), for the temperature node P_d of the non-meshing surface, the incoming heat flow from the temperature node P_c is equal to the outcoming heat flow to the tooth space. Q_{1i} is the frictional heat flux of the i-th discrete area of Gear 1 (unit: W/mm^2); S_{1i} is the contact area of the i-th discrete area of Gear 1 (unit: mm^2); T_{ci} is the temperature value of the meshing flank temperature node P_a of the i-th discrete area of Gear 1 (unit: °C); T_{li}, T_{ri} are the temperature values of temperature nodes P_b or P_c respectively for the i-th discrete area of Gear 1 (unit: °C); T_{ni} is the temperature value of the non-meshing flank temperature node P_d of the i-th discrete area of Gear 1 (unit: °C); R_{ci} is the thermal resistance of heat convection of meshing flank temperature node P_a of the i-th discrete area of Gear 1 (unit: °C/W); R_{ni} is the thermal resistance of heat convection of non-meshing flank temperature node P_a of the i-th discrete area of Gear 1 (unit: °C/W); $R_{lt}?AR_{rt}$ is the thermal resistance of heat convection of the addendum face temperature node P_a of the i-th discrete area of Gear 1 (unit: °C/W); R_{lhi} is the thermal resistance of heat conduction in the i-th discrete area of Gear 1 between temperature node P_a and P_b (unit: °C/W); R_{mhi}, R_{rhi}, R_{lvi}, $R_{lv(i+1)}$, R_{rvi}, $R_{rv(i+1)}$ is the thermal resistance of heat conduction in the i-th discrete area of Gear 1 between temperature node P_b and P_c, P_c and P_d, P_b and P_e, P_b and P_g, P_c and P_f, P_c and P_h respectively (unit: °C/W).

$$
\begin{cases}
Q_{11}S_{11} = \dfrac{T_{c1}-T_a}{R_{c1}} + \dfrac{T_{c1}-T_{l1}}{R_{lh1}} \\
\dfrac{T_{c1}-T_{l1}}{R_{lh1}} = \dfrac{T_{l1}-T_a}{R_{lv1}+R_{lt}} + \dfrac{T_{l1}-T_{r1}}{R_{mh1}} + \dfrac{T_{lc1}-T_{lc2}}{R_{lv2}} \\
\dfrac{T_{l1}-T_{r1}}{R_{mh1}} = \dfrac{T_{rc1}-T_a}{R_{rv1}+R_{rt}} + \dfrac{T_{r1}-T_1}{R_{rh1}} + \dfrac{T_{r1}-T_{r2}}{R_{rv2}} \\
\dfrac{T_{r1}-T_{n1}}{R_{rh1}} = \dfrac{T_{n1}-T_a}{R_{n1}} \\
\vdots \\
Q_{1n}S_{1n} = \dfrac{T_{cn}-T_a}{R_{cn}} + \dfrac{T_{cn}-T_{ln}}{R_{lhn}} \\
\dfrac{T_{cn}-T_{ln}}{R_{lhn}} = \dfrac{T_{ln}-T_{l(n-1)}}{R_{lvn}} + \dfrac{T_{ln}-T_{rn}}{R_{mhn}} + \dfrac{T_{ln}-T_{l(n+1)}}{R_{lv(n+1)}} \\
\dfrac{T_{ln}-T_{rn}}{R_{mhn}} = \dfrac{T_{rn}-T_{r(n-1)}}{R_{rvn}} + \dfrac{T_{rn}-T_{nn}}{R_{rhn}} + \dfrac{T_{rn}-T_{r(n+1)}}{R_{rv(n+1)}} \\
\dfrac{T_{rn}-T_{nn}}{R_{rhn}} = \dfrac{T_{nn}-T_a}{R_{nn}}
\end{cases}, \tag{14}
$$

According to the rules in (10) to (13), totally $4n$ equations can be listed for n discrete areas, which are shown in (14). The friction heat flux is calculated according to the equations given in Mao [6]. The calculations of thermal resistance in the gear temperature field using the thermal network method are referred to Gou [20]. When calculating the thermal resistance of heat convection of Gear 1, is required to solve the heat convection coefficient h_a of Gear 1 meshing flank. As described in Handschuh [21], the meshing flank can be simplified as the heat convection between the meshing flank and the lubricating oil.

The calculations of thermal resistance in gear temperature field using the thermal network method are referred to the equations given in Zhou [15]. The thermal resistances (unit: °C/W) of the meshing face and the non-meshing face need to be calculated, including the thermal resistance

of heat convection to tooth space R_{ci}, R_{ni}, the thermal resistance of addendum heat convection R_{lt}, R_{rt}, and the thermal resistance of heat conduction inside the tooth body R_{lhi}, R_{mhi}, R_{rhi}, R_{lvi}, R_{rvi}.

$$R_{ci} = 1/(h_a \cdot l_i \cdot b), \tag{15}$$

$$R_{ni} = \frac{1}{(h_c \cdot l_i \cdot b)}, \tag{16}$$

$$R_{lt} = R_{rt} = 1/(h_b \cdot (s_{1i}/2) \cdot b), \tag{17}$$

$$R_{lhi} = R_{mhi} = R_{rhi} = \frac{h_i}{\left(l_i \cdot \left(\frac{s_{1i}}{3}\right) \cdot k\right)}, \tag{18}$$

$$R_{lvi} = R_{rvi} = \frac{l_i}{\left(\left(\frac{s_{1i}}{2}\right) \cdot b \cdot k\right)}, \tag{19}$$

where h_a and h_c are the coefficients of heat convection of the meshing face and the non-meshing face (unit: W/(mm^2·°C)); l_i is the length of the meshing flank and the non-meshing flank corresponding to the i-th discrete area of Gear 1 (unit: mm); s_{1t} is the thickness of the addendum of the Gear 1 (unit: mm); k is heat transfer coefficient of the material of Gear 1 (unit: W/(mm·°C)).

2.3. Friction heat flux

The friction heat flux is calculated according to the equations given in Mao [6]. The friction heat flux Q_{1i} (unit: W/mm^2) of Gear 1 is determined by average Hertz contact stress $\overline{p}_{1i}$ (unit: N) at any meshing point on the meshing face of Gear 1, relative sliding velocity v_{12i} (unit: mm/s) of any meshing point of the meshing face, friction coefficient of Gear 1 meshing face f, the distribution coefficient of heat flux between teeth q_{1i} and the gear meshing time t_{1i} (unit: s) of any meshing point of Gear 1, which is described in (20).

$$Q_{1i} = \overline{p}_{1i} f v_{12i} q_{1i} t_{1i}, \tag{20}$$

$$t_{1i} = \frac{2a_{1i}}{v_{1i}} \cdot \frac{60}{n_1}, \tag{21}$$

where n_1 is the rotation speed of Gear 1 (unit: rpm); a_{1i} is the Hertz semi-contact width of Gear 1 (unit: mm); v_{1i} is tangential velocity of Gear 1 in any meshing point (unit: mm/s).

The relative sliding speed of any meshing point of the gear and the characteristics of the gear materials are different, therefore, the friction heat flux distribution is unbalanced. When the materials of Gear 1 and Gear 2 are the same, the distribution coefficient of friction heat flux q_{1i} between teeth is established, as shown in (22).

$$q_{1i} = \frac{\sqrt{v}_{1i}}{\sqrt{v}_{1i} + \sqrt{v}_{2i}}. \tag{22}$$

The average Hertz contact stress $\overline{p}_{1i}$ of any meshing points in the meshing face of Gear 1 and the Hertz semi-contact width of Gear 1 a_{1i} are shown in (23) and (24) respectively.

$$\overline{p}_{1i} = \frac{\pi}{4}\sqrt{\frac{F_{n1i}E_e}{2\pi R_i b_1}}, \tag{23}$$

$$a_i = \sqrt{\frac{8F_{n1i}R_i}{\pi E_e b}}, \tag{24}$$

$$S_{1i} = 2 \cdot a_i \cdot b, \tag{25}$$

where F_{n1i} is the normal force of any meshing points in the meshing face of Gear 1 (unit: N); E_e is the elastic module of Gear 1 and Gear 2 (unit: Pa); R_i is the equivalent curvature radius of gear meshing point (unit: mm); b is the tooth width (unit: mm); S_{1i} is the contact area of any meshing point of Gear 1 (unit: mm^2).

When a pair of gear is in meshing, the radius of curvature of driving Gear 1 continues to increase, and the radius of curvature of driven Gear 2 continues to decrease. The equivalent curvature radius at any gear meshing point is shown in (27) and (28).

$$R_c = \frac{R_{1i}R_{2i}}{R_{1i} + R_{2i}}, \tag{26}$$

$$R_{1i} = r_{b1} \tan \alpha_i, \tag{27}$$

$$R_{2i} = L_N - R_{1i}, \tag{28}$$

where R_{1i} and R_{2i} are the radii of curvature of Gear 1 and Gear 2 respectively at any meshing point on the tooth face (unit: mm); α_i is pressure angle of any meshing point on the gear meshing face (unit: rad); L_N is the length of gear meshing line (unit: mm).

To obtain the relative sliding velocity v_{12i} of the gear meshing point, as shown in (29), the Gear 1 and Gear 2 rotation velocity ω_1 and ω_2 need to be determined respectively, and then the difference of tangential velocity is calculated.

$$v_{12i} = |R_{1i}\omega_1 - R_{2i}\omega_2| \tag{29}$$

2.4. Deformation on the gear meshing line influenced by temperature

Regarding the proposed deformation on the gear meshing line of Gear 1 and Gear 2 caused by temperature, the thermal deformation of each discrete area along the x and y direction need to be converted into the direction of gear meshing line, as shown in Fig. 5. As an example, the δ_{1BDi} is calculated, which is the thermal deformation of the gear meshing line in the single tooth meshing area BD in the i-th discrete area of Gear 1. The thermal deformation of the i-th discrete area in the x and y direction δ_{t1xi} and δ_{t1yi} need to be calculated first, then transformed to the meshing line and combined to be δ_{1BDi}, and the equation is expressed in (30). The angle between the line segment FG and the gear meshing line φ_{1Ni} is calculated as (33).

$$\delta_{1BDi} = \delta_{t1xi} \cos \varphi_{1Ni} + \delta_{t1yi} \sin \varphi_{1Ni} \tag{30}$$

$$\delta_{t1xi} = L_{FG}, \tag{31}$$

$$\delta_{t1yi} = L_{FH}, \tag{32}$$

$$\varphi_{1Ni} = \alpha_i - \xi_{1i}, \tag{33}$$

where δ_{t1xi}, δ_{t1yi} is the thermal deformation in the direction x or y of Gear 1 respectively (unit: mm); φ_{1Ni} is the angle between the line segment FG and the gear meshing line (unit: rad); α_i is the pressure angle of any meshing point of each discrete area (unit: rad); ξ_{1i} is the angle between the line of the radius connected from the i-th meshing point of Gear 1 to the centre of the base circle of Gear 1 and the y-axis (unit: rad).

Metrol. Meas. Syst., Vol. 31 (2024), No. 1, pp. 3–21
DOI: 10.24425/mms.2024.148543

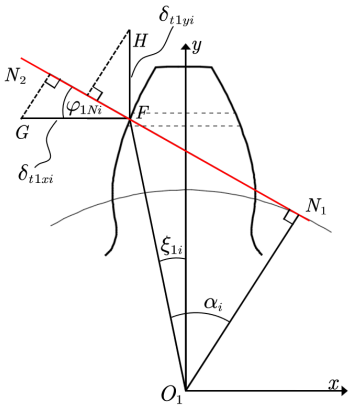

Fig. 5. The deformation on the meshing line caused by temperature.

A gear tooth is divided into three sections: involute section, root fillet section and dedendum section. For the involute section, which is discretized into several regions, and the thermal deformation δ_{t1xi} and δ_{t1yi} in the x and y directions of the i-th discrete area is obtained in Eqs. (34) and (35). For the root fillet section and the dedendum section, only the thermal deformation in the y direction needs to be calculated as in (36) and (37).

$$\delta_{t1xi} = 0.5\,(\delta_{txli} + \delta_{txri}), \tag{34}$$

$$\delta_{t1yi} = 0.5 * \left(\delta_{tyli} + \delta_{1c} + \delta_{1f}\right) + 0.5 * (\delta_{tyri} + \delta_{1c} + \delta_{1f}), \tag{35}$$

$$\delta_{1c} = h_{1c} \cdot T_a \cdot \lambda, \tag{36}$$

$$\delta_{1f} = h_{1f} \cdot T_a \cdot \lambda, \tag{37}$$

where δ_{txli}, δ_{tyli}, δ_{txri}, δ_{tyri} is respectively the thermal deformation in the left and right direction on x and y axis of the i-th discrete area (unit: *mm*); h_{1c} is the height in the y direction of root fillet (unit: mm); T_a is ambient temperature (unit: °C); λ is the coefficient of thermal expansion (unit: 1/°C); h_{1f} is the height in the y direction of root (unit: mm).

For the involute section, considering the i-th discrete area, the deformations δ_{txli}, δ_{txri}, δ_{tyli}, δ_{tyri} are described in (38) to (41). In these equations, T_{ci}, T_{li}, T_{ri}, T_{ni} are the related temperatures in the i-th discrete area of Gear 1 in the gear temperature field distribution model based on the thermal network method as shown in Fig. 5.

$$\delta_{txli} = \frac{s_i}{2} \cdot \Delta T_{li} \cdot \lambda, \tag{38}$$

$$\delta_{tyli} = \sum_{i}^{n} (h_i \cdot \Delta T_{li} \cdot \lambda), \tag{39}$$

$$\delta_{txri} = \frac{s_i}{2} \cdot \Delta T_{ri} \cdot \lambda, \tag{40}$$

$$\delta_{tyri} = \sum_{i}^{n} (h_i \cdot \Delta T_{ri} \cdot \lambda), \tag{41}$$

$$\Delta T_{li} = T_{ci} + T_{li} - T_s, \tag{42}$$

$$\Delta T_{ri} = T_{ni} + T_{ri} - T_s, \tag{43}$$

where T_s (20°C) is standard temperature.

Based on the analysis above, the deformation of the gear meshing line caused by temperature for the i-th discrete area of Gear 1 is obtained by (30). For n discrete areas, the variation of deformation $\Delta\delta_{1BD}$ is proposed as in (30).

$$\Delta\delta_{1BD} = \sum_{1}^{n} \left(\delta_{t1xi} \cos\varphi_{1Ni} + \delta_{t1yi} \sin\varphi_{1Ni}\right) + \sum_{1}^{n} \left(\delta_{t2xi} \cos\varphi_{2Ni} + \delta_{t2yi} \sin\varphi_{2Ni}\right) \tag{44}$$

where δ_{t1xi}, δ_{t1yi}, δ_{t2xi}, δ_{t2yi} is the thermal deformation on x or y axis of the i-th discrete area of Gear 1 or Gear 2 respectively (unit: mm) φ_{1Ni}, φ_{2Ni} is the angle between the line segment FG and the meshing line of Gear 1 and Gear 2 respectively (unit: rad).

3. Numerical analysis

3.1. Variation of gear transmission errors for different temperatures

Numerical simulation based on (29) is processed in MATLAB, and the variation of transmission errors (TEs) within a single pitch angle under different temperatures are obtained. The gear material parameters Cr12Mov are listed in Table 1, and the gear parameters are shown in Table 2. The numerical simulations are carried out under the same conditions except for the temperature. The speed of Gear 1 is 1000 rpm and that of Gear 2 is 680 rpm, the input torque of Gear 1 is 1 N·m, and the parameters of the lubrication oil are given in Table 3 [22]. The temperatures are divided into 11 groups from 0°C–100°C with a step of 10°C.

Temperature 20°C is referred to as the standard temperature. The variations of gear TEs between other temperatures and standard temperature are calculated. Along the meshing line, the direction is defined as positive according to the external direction of the Gear 1 tooth-flank.

Table 1. Gear material parameters.

Material parameters (Cr12Mov)	**Gear 1**	**Gear 2**
Elastic modulus (Pa)	2.06e11	2.06e11
Poisson's ratio	0.3	0.3
Coefficient of heat conductivity (W/mm·K)	48	48
Density (g/cm^3)	7.9	7.9
Specific heat capacity J/(kg·°C)	502.4	502.4
Coefficient of thermal expansion (1/°C)	1.1e-5	1.1e-5

Table 2. Gear parameters.

Parameters	**Gear 1**	**Gear 2**
Module (mm)	0.8	0.8
Tooth number	17	25
Pressure Angle (°)	20	20
Tooth width (mm)	5	5
Tip clearance coefficient	0.25	0.25
Addendum coefficient	1	1

Metrol. Meas. Syst., Vol. 31 (2024), No. 1, pp. 3–21
DOI: 10.24425/mms.2024.148543

Table 3. Lubricating oil parameters (60°C) [22].

Parameter	Value
Coefficient of heat conductivity (W/mm·K)	0.1446
Density (g/cm^3)	0.8690
Specific heat capacity J/(kg·°C)	2114
Kinematic viscosity (m^2/s)	50.5
Prandtl number	462

The gear meshing will take place in advance because of gear thermal expansion, which results in reduction of φ_2' and gear TEs. The variation of transmission errors is 1.05 μm at °C, while the variation is −4.20 μm at 100°C in Fig. 6. The variation of the gear transmission error caused by temperature is of the order of μm, and the variation of the gear backlash [23] is smaller than that of the gear transmission error.

The variation of *transmission errors* (TEs) for this temperature is defined as the mean value of the variation of TEs of Gear 1 along its rotation angle for a given temperature compared to the TEs at the standard temperature 20°C. The relationship between the variation of TEs and the temperature can be observed in Fig. 7, and the values are listed in Table 4. It can be found that as the temperature increases from 0°C to 100°C, the variation of gear TEs decreases along the negative direction and keeps the linear relationship, that is to say, the absolute value of variation of gear TEs is larger while the temperature is higher.

Table 4. Variations of gear transmission errors under different temperatures in TETN (μm).

Temp. (°C)	Vari. (μm)	Temp. (°C)	Vari. (μm)	Temp. (°C)	Vari. (μm)
0	1.05	40	–1.05	80	–3.15
10	0.52	50	–1.58	90	–3.67
20	0	60	–2.10	100	–4.20
30	–0.53	70	–2.62	–	–

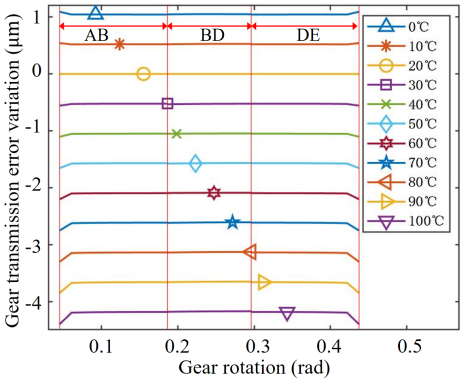

Fig. 6. Variation of gear TEs at different temperatures in TETN.

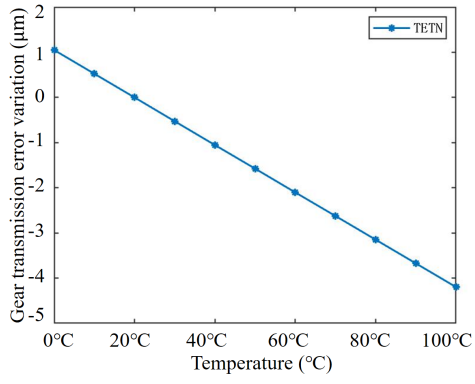

Fig. 7. Relation between temperature and variation of TEs in TETN.

3.2. Variation of gear transmission errors in different materials

The deformation in materials caused by temperature will be proportionate to their coefficient of thermal expansion, which will influence gear TEs. Numerical simulations of gear TEs for different materials are carried out below.

The gear parameters used in the numerical simulations are the same as in Table 2. The related conditions in simulations are as follows: the temperature is 60°C, the speed of Gear 1 is 1000 rpm, the speed of Gear 2 is 680 rpm, the input torque of Gear 1 is 1 N·m, the parameters of the lubricating oil are shown in Table 3, and the materials are listed in Table 5.

Table 5. Variation of gear transmission errors for different materials μm.

Material	Coef. of thermal expansion (1/°C)	Variation (μm)
Cr12MoV	1.09e-5	–2.08
20Cr	1.13e-5	–2.16
45 Steel	1.159e-5	–2.22
60Si2Mn	1.195e-5	–2.29
40CrMnSiMoA	1.25e-5	–2.39
38CrA	1.34e-5	–2.56

Figure 8 shows the results of numerical simulation for the variation of TEs of a single pitch angle for different materials. The absolute value of the variation of TEs of gear with material Cr12MoV being the smallest; while the material 38CrA is the biggest.

The variation of *transmission errors* (TEs) for a certain material is defined as the mean value of the variation of TEs of Gear 1 along its rotation angle for this material compared to the TEs at the standard temperature. The relationship between material thermal expansion coefficients and the variation of gear TEs is shown in Fig. 9, and the values are listed in Table 5. It can be observed that as the coefficients of thermal expansion of gear material increases, so does the absolute value of the variation of transmission errors, and the relationship is approximately linear.

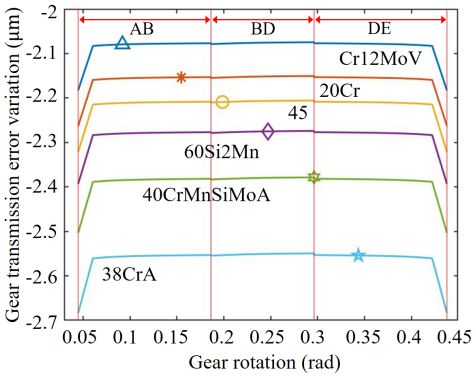

Fig. 8. Variation of gear TEsfor different materials.

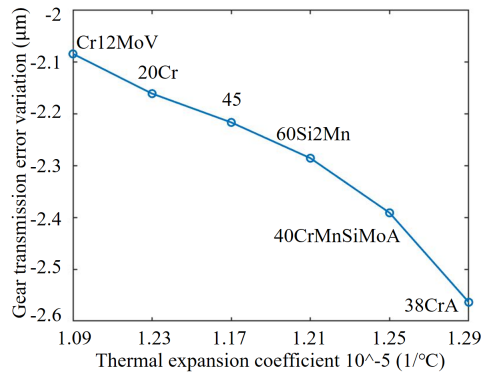

Fig. 9. Relation between material thermal expansion coefficients and the variation of gear TEs.

4. Simulations in Workbench for gear temperature field and the TE

4.1. Simulation of the gear temperature field

Workbench is a finite element simulation software under the Ansys software, which can be used in temperature field and structural analysis. Ansys Workbench version 19.2 was used in the simulation. As analysed in Section 2.2, the bulk temperature field of a single tooth is analysed.

In the temperature field simulation, the gears are divided into several regions. The heat flux and heat convection in each region are obtained by calculating the equations in Section 2.2 and then applied to each region respectively. After setting other simulation conditions, the finite element simulation results are obtained.

In the finite element simulation of the influence of temperature on gear transmission error, the above temperature field simulation results are applied to the gear structure simulation as loads and other boundary conditions are added. According to the gear parameters shown in Table 1, he grids of meshing a single tooth are divided in the finite element pre-processing software Hypermesh under Hyperworks. The division element type is Solid278. In order to reduce the calculation time, the tooth flank is divided into refined grids, which have 8064 nodes and 6720 elements. The meshing results are shown in Fig. 10. After it is imported into Workbench, the bulk temperature field is analysed using the State Thermal Module.

Frictional heat flux Q_{1i} and the coefficient of heat convection h_a for the meshing tooth flank need to be input as well as the coefficient of heat convection h_b for the gear end face and tip surface, and the coefficient of heat convection h_c of the non-meshing flank and root face.

The gear temperature field of a single tooth is analysed as shown in Fig. 11. The maximum temperature appears at the initial mesh area and the separate mesh area, because in those areas the relative sliding speed is higher, the frictional heat flux is relatively bigger, and the temperature is higher. In the same contact area, the temperature near the end face is lower and the temperature of the middle area in the tooth width is higher. That is why the coefficient of heat convection of the end face is bigger, therefore, the closer to the end face, the faster the heat flow will be dissipated, while the coefficient of heat convection of middle part is smaller.

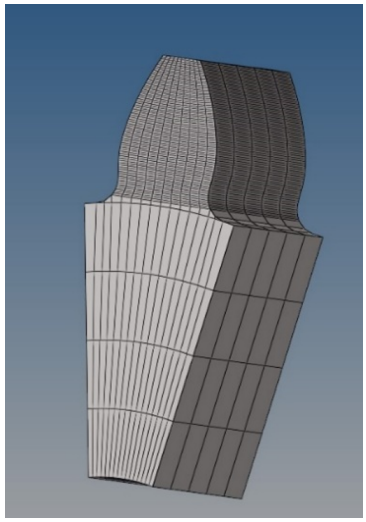

Fig. 10. Tooth grids.

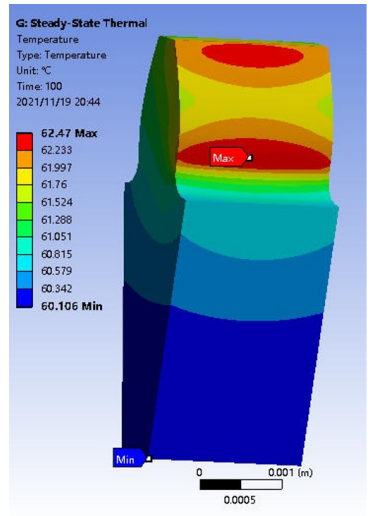

Fig. 11. Temperature field.

4.2. Temperature comparison on the gear meshing line

The temperature value of T_{ci} in the gear temperature field distribution model based on the *thermal network method* (TFD-TN) according to (14) is compared to the extracted temperature value at the middle node of the tooth width in the gear bulk temperature field analysis by the FEM method in Section 4.1. The comparison results are shown in Fig. 13. The temperature obtained by T_{ci} in the TFD-TN temperature model gradually decreases on the meshing line in the first gear double-teeth meshing area AB, and the temperature reaches the maximum value at the initial meshing position, where the relative slide velocity is maximum.

In the single-tooth meshing area BD, the number of contact points changes from two to one, the normal stress of the gear meshing flank and the frictional heat flux increase. But when the gear meshing point moves to the C, the relative sliding speed and the frictional heat flux is 0, and the temperature of node C reaches the minimum value. As the gear continues to rotate, due to the increase of the relative slide velocity, the frictional heat flux and the temperature increases on the gear meshing line.

After the gear enters the second double-teeth meshing area DE, the number of contact point changes from one to two, and the contact stress decreases. However, as the gear rotates, the relative slide velocity and the friction heat flux increase, the temperature on gear meshing line rises gradually.

In Fig. 12, the results yielded by the TFD-TN model and those of the FEM have the same decreasing trend in the first double-teeth meshing zone AB. The results of the TFD-TN model drop first and then rise in the single-tooth meshing zone BD, the lowest temperature value occurs at the node C, and the temperature rises again in the second double-teeth meshing zone DE.

The average difference of the TFD-TN results as compared to the FEM result is -0.12°C, and the maximum difference is 1.01°C. This is because in the finite element analysis, between adjacent temperature nodes, the node with higher friction heat flux transfers heat to the node with lower one, which will cause the maximum temperature to be lowered, and the lower temperature to be raised. Therefore, the TFD-TN temperature model proposed can be referred to in a certain range.

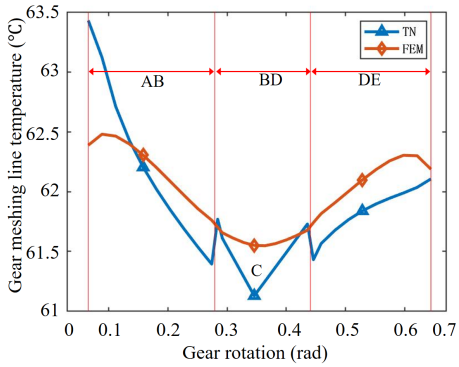

Fig. 12. Comparison of results.

4.3. Simulations for gear transmission errors

After completing the gear temperature field analysis, the results are used as the load in simulation of the gear transmission error. Grid partitioning of the simplified gear model is performed in Hypermesh. The element type is Solid185. The gear model is divided into refined

grids, which have 62244 nodes and 45936 elements, as shown in Fig. 13. The contact state should be set to single-flank meshing, and the coefficient of friction of the contact flank is set as 0.05.

The finite element simulations of gear transmission errors for different temperatures are next carried out. The revolution speed of Gear 1 is 1000 rpm, and that of Gear 2 is 680 rpm, the torque is 1 N·m. There are 11 groups of temperatures ranging from 0°C to 100°C. The other conditions remain the same. The simulation results for gear transmission errors are shown in Fig. 14. As the temperature rises, the values of gear transmission error decrease, but the differences between the peak and valley values change little with temperature. Following the definition in Section 3.1, the values of the variation of transmission errors and the temperature in FEM are listed in Table 6.

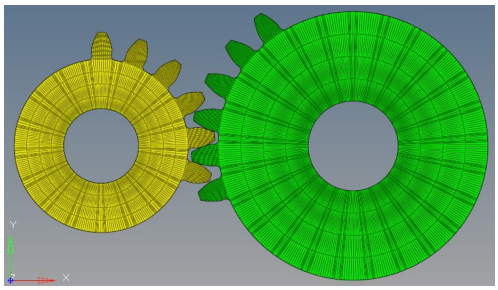

Fig. 13. Gear model meshing.

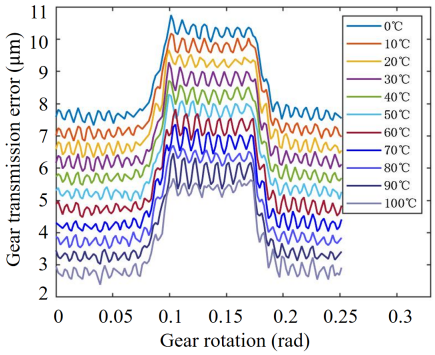

Fig. 14. TE results in FEM.

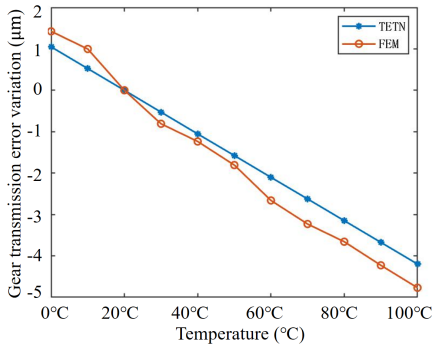

Fig. 15. Comparison of TETN and FEM.

Table 6. Variations of gear transmission errors for different temperatures in FEM (μm).

Temp. (°C)	Vari. (μm)	Temp. (°C)	Vari. (μm)	Temp. (°C)	Vari. (μm)
0	1.42	40	–1.24	80	–3.66
10	1.00	50	–1.81	90	–4.23
20	0	60	–2.66	100	–4.77
30	–0.81	70	–3.23	–	–

4.4. Comparison of gear transmission error variation

The gear transmission error variations for different temperatures as the numerical results of the TETN model listed in Table 4 and results analysed by the FEM listed in Table 6 are compared. The difference Δ_1 is shown in Fig. 15, and the values are listed in Table 7. The maximum difference of

TETN model compared to the FEM method is 0.61 μm, while the average difference is 0.24 μm. The gear transmission error variations using the TETN model proposed are close to the results by the FEM method.

Table 7. The difference between TETN and FEM.

Temp. (°C)	Δ_1 (μm)	Temp. (°C)	Δ_1 (μm)	Temp. (°C)	Δ_1 (μm)
0	–0.37	40	0.19	80	0.51
10	–0.48	50	0.23	90	0.56
20	0	60	0.56	100	0.57
30	0.28	70	0.61	–	–

5. Experiments concerning the influence of temperature on transmission errors

As the last stage of the study, experiments were carried out with the use of a gear tester transmission performance tester with controlled temperature. As shown in Fig. 16, it is composed of a test bench, a console and a temperature control box. Circular gratings are used in the power input end and the power output end to measure the input and output rotation angles.

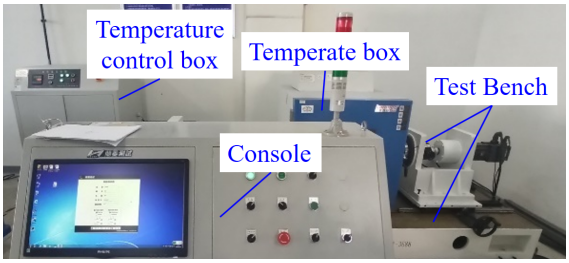

Fig. 16. Gear transmission performance tester with temperature simulation.

The temperature box keeps the measurand at the assigned ambient temperature. The measurand in this experiment is a two-stage planetary reducer. The input of both two stages of planetary gears is the sun gear, and the output is the planet carrier. Only the temperature condition changes in the experiments. Seven data sets were obtained within the temperature range of 0°C to 100°C.

In the test, the ambient temperature of the gear is first controlled as the set temperature, which is determined after the temperature measurement by the sensor, and then the test is carried out. In order to ensure that the measurement is carried out at the same position as much as possible, at the end of each test, the same angle is reversed to the original position. The transmission error curves of planetary reducer are shown in Fig. 17.

In order to compare the numerical results of the TETN model with the experimental results, the error transfer relationship along the line of action needs to be considered. The variation of gear transmission errors by temperature obtained through the TETN model proposed is converted into the value of the two-stage gear reducer using (45). The first and second gear parameters of the two-stage reducer are all the same as the gear parameters in Table 2. The transmission ratio between the two stages is $i_{12} = 1.47$.

$$\Delta TE = \Delta TE_2 + i_{12}\Delta TE_1, \tag{45}$$

where ΔTE is the variation of transmission error of the two-stage gear reducer under the influence of temperature (unit: μm); ΔTE_1, ΔTE_2 is the variation of transmission error of the first-stage, second-stage gear reducer under the influence of temperature respectively (unit: μm).

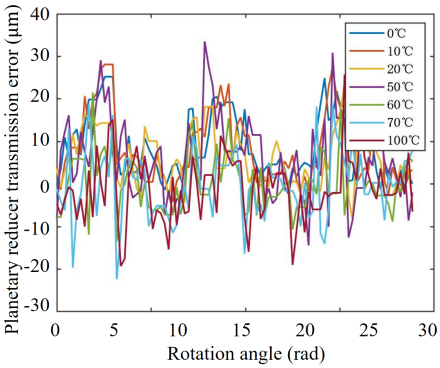

Fig. 17. TE curves in the tester.

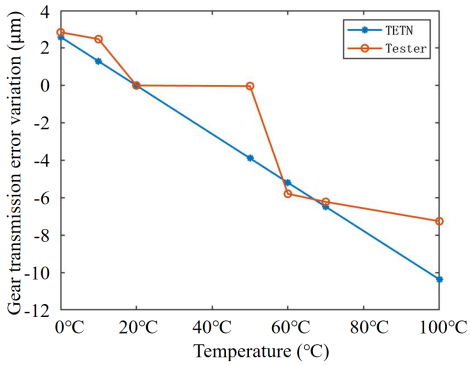

Fig. 18. Comparison of TETN and the tester.

For the measurement results in the tester, the variation of transmission error (as defined in Section 3.1) for different temperatures is obtained. The converted TETN model results using (45) based on the results in Table 4 are compared with the measurement results of the tester, as shown in Fig. 18, and the variations of transmission errors at different temperatures are the results obtained by subtracting the transmission errors at 20 °C from the transmission errors at other temperatures. The curves can show that the value of the variation of transmission errors by two methods is relatively close and the variation trend is consistent. The results of transmission error variation by the TETN model compared with the experimental results is −1.15 μm. The reasons for the differences between the experimental and simulation results may include the temperature control and the uncertainty of the tester. Therefore, the TETN model proposed in this paper can be used to evaluate the influence of temperature on gear transmission error within a certain range.

6. Conclusions

To solve the problem of gear transmission performance influenced by the ambient temperature, considering the gear single-flank meshing progress, the model of influence on cylindrical gear *transmission errors by temperature based on the thermal network* (TETN) is established. To obtain the relationship between temperature and the variation of gear transmission errors, the model must include establishing the distribution of the gear bulk temperature field based on thermal network method and analysis of the deformation along of the gear meshing line caused by temperature.

Based on the TETN model proposed, the variation of gear transmission errors within range of 0 °C to 100 °C is obtained in MATLAB. The variation of gear transmission error at 100 °C relative to 20 °C is −4.20 μm. The variation of gear transmission errors for a certain temperature with different materials is calculated. Gear temperature field and gear transmission errors are then simulated using the *Finite Element Method* (FEM) by Workbench 19.2 of Ansys. The results of transmission error variation by the TETN model are compared with the simulation results of FEM, the average difference is 0.24 μm. The experiments are carried out on the gear transmission performance tester with temperature simulation. The average difference of the TETN model results compared to the experimental results is −1.15 μm.

The distribution model of gear bulk temperature field based on the thermal network provides a method for gear temperature field analysis. It is observed that the variation of gear transmission errors is approximately linear with temperature, and the main reason is that the thermal deformation of gear material caused by temperature is linear. Concerning that the results are close to and consistent with the simulation results of FEM and the experimental results of the tester, the TETN model proposed can be used to determine the variation of gear transmission errors under the influence of temperature, as well as provide a basis for analysing the gear transmission errors for different temperatures.

Acknowledgements

This research was supported by the National Key R&D Program of China (Project No. 2017YFF0204804).

References

[1] Munro, R. G. (1979). A review of the single flank method for testing gears. *CIRP Annals – Manufacturing Technology*, 28, 325–329.

[2] Smith, R. E. (2004). Single-flank testing of gears. *Gear Technology*, 21, 18–21.

[3] Blok, H. (1963). The flash temperature concept. *Wear*, 6, 483–494.

[4] Taburdagitan, M., & Akkok, M. (2006). Determination of surface temperature rise with thermo-elastic analysis of spur gears. *Wear*, *261*(5–6), 656–665. https://doi.org/10.1016/j.wear.2006.01.019

[5] Li, S., & Anisetti, A. (2016). On the flash temperature of gear contacts under the tribo-dynamic condition. *Tribology International*, *97*, 6–13. https://doi.org/10.1016/j.triboint.2016.01.027

[6] Mao, K. (2007). A numerical method for polymer composite gear flash temperature prediction. *Wear*, *262*(11–12), 1321–1329. https://doi.org/10.1016/j.wear.2007.01.008

[7] Li, J., Zhang, L., & Zhao, Q. (2009). Finite element modeling and analysis on interfacial contact temperature of gears based on Ansys. *10th IEEE International Conference on Computer-Aided Industrial Design and Conceptual Design*, 668–673. https://doi.org/10.1109/CAIDCD.2009.5375000

[8] Shi, Y., Yao, Y. P., & Fei, J. Y. (2016). Analysis of bulk temperature field and flash temperature for locomotive traction gear. *Applied Thermal Engineering*, *99*, 528–536. https://doi.org/10.1016/j.applthermaleng.2016.01.093

[9] Wang, S. S., Wang, S. K., Wang, J., & Deng X. Q. (2020). Temperature field simulation and experimental study of anti-backlash single-roller enveloping hourglass worm gear. *Chinese Journal of Mechanical Engineering*, *33*, 1–10. https://doi.org/10.1186/s10033-020-00475-x

[10] Yi, J., & Quinonez, P. D. (2005). Gear surface temperature monitoring. *Proceedings of the Institution of Mechanical Engineers Part J-Journal of Engineering Tribology*, *219*, 99–105. https://doi.org/10.1243/135065005X9745

[11] Miltenovic ,A., Tica, M., Banic, M., & Miltenovic, D. (2020). Prediction of temperature distribution in the worm gear meshing. *Facta Universitatis, series: Mechanical Engineering*, *18*(2), 329–339. https://doi.org/10.22190/FUME180120016M

[12] Roda–Casanova, V., & Sanchez–Marin, F. (2019). A 2D finite element based approach to predict the temperature field in polymer spur gear transmissions. *Mechanism and Machine Theory*, *133*, 195–210. https://doi.org/10.1016/j.mechmachtheory.2018.11.019

[13] Li, W., Zhai, P. F., Tian, J. Y., & Luo, B. (2018). Thermal analysis of helical gear transmission system considering machining and installation error. *International Journal of Mechanical Sciences*, *149*, 1–17. https://doi.org/10.1016/j.ijmecsci.2018.09.036

[14] Blok, H. (1995). Thermal network for predicting bulk temperature in gear transmissions. *Proc.7th Round Table Discussion, Marin Reduction Gears, Fins pong, Sweden*, 21–25.

[15] Zhou, C. J., Xing, M. C., Wang, H. B., & Hu, B. (2021). A novel thermal network model for predicting the contact temperature of spur gears. *International Journal of Thermal Sciences*, *161*, 06703. https://doi.org/10.1016/j.ijthermalsci.2020.106703

[16] Wiemann, A. K., Stein, M., & Kniel, K. (2019). Temperature influence on involute gear measurements. *Engineering Research*, *83*, 683–690. https://doi.org/10.1007/s10010-019-00346-5

[17] Wang, C. (2019). A calculation method of thermal deformation for double helical gear. *Mechanics and Industry*, *20*(6), 612. https://doi.org/10.1051/meca/2019045

[18] Trochta, M., Folta, Z., & Burian, M. (2014). Contribution to the methodology of measuring transmission error. *55th International Conference of Machine Design Departments*, 503–507.

[19] Wang, Y. N., Sun, Z. L., & Yin, M. A. (2013). Considering thermal deformation in gear transmission error calculation. *Applied Mechanics and Materials*, *281*, 211–215. https://doi.org/10.4028/www.scientific.net/AMM.281.211

[20] Gou, X. F., Zhu, L. Y., & Qi, C. J. (2017). Nonlinear dynamic model of a gear-rotor-bearing system considering the flash temperature. *Journal of Sound and Vibration*, *410*, 187–208. https://doi.org/10.1016/j.jsv.2017.08.014

[21] Handschuh, R. F., & Kicher, T. P. (1996). Method for thermal analysis of spiral bevel gears. *Journal of Mechanical Design*, 118, 580–585.

[22] Zhao, Z. N. (2008). Heat Transfer. *Beijing: Chemical Industry Press*, *473*. (in Chinese)

[23] Lu R, & Tang W. (2022). Analytical calculation models for mesh stiffness and backlash of spur gears under temperature effects[J]. *Proceedings of the Institution of Mechanical Engineers, Part C: Journal of Mechanical Engineering Science*, *236*(8): 4450–4462. https://doi.org/10.1177/09544062211049860

Jie Tang received her B.Sc. degree in 1998 from Southeast University and her Ph.D. degree in 2009 from Beijing University of Technology. She is currently an Associate Professor at Beijing University of Technology. She specializes in precision measurement technology and instruments and gear metrology.

Heng Guo is a graduate student at Beijing University of Technology. He specializes in precision measurement technology and instruments.

Hui Wan is a graduate student at Beijing University of Technology. He specializes in precision instrument and mechanism.